International Journal of Enhanced Research in Science, Technology & Engineering
ISSN: 2319-7463, Vol. 4 Issue 9, September-2015

Seismic image enhancement in complex structures by introducing CO-CDS stack method

A. Shahbazi[1*], D. Ghosh[2], M. Soleimani[3], A. Gerami[4]

[1,2,4]Faculty of Petroleum Geoscience, Universiti Teknologi, PETRONAS, Malaysia
[3]Assistant Professor, Faculty of Mining, Petroleum and geophysics, University of Shahrood, Shahrood, Iran

ABSTRACT

Seismic imaging in complex or semi-complex structures is a problematic issue due to possible strong lateral velocity changes and existence of conflicting dips. There are several methods for resolving these problems. However, some methods, like as the reverse time migration (RTM), the full waveform inversion (FWI) and the common reflection surface, (CRS) have got some drawbacks in application for complex structures. In this study, the problem of imaging in complex structures is going to be resolved by improving the CRS method into a diffraction mode in common offset manner, which could be called, the Common Offset Common Diffraction Surface (CO-CDS) method. To modify the CO-CRS travel time equation into the CO-CDS equation, the imaginary shot reflector idea in the CRS, which produce a reflection surface, should be changed to a diffraction point. Thus the CO-CRS equation, which is based on five kinematic wavefield attributes, should be modified to satisfy the diffractor point on the reflector. Two attributes of the CO-CRS equation are related to source and receiver's central ray emerging angles and the rest are related to radius of normal and normal incidence point (NIP) waves, again in source and receivers. In the CO-CDS stack equation, the two wavefronts which reach the receivers, have to be equal. The CO-CDS equation was derived based on these facts and the shape of operator was changed, too. By this equation, each point of the reflector is imaged like as conventional diffraction stack migration, by preserving advantages of CRS method. The synthetic Sigsbee 2A data and a real complex data were imaged by this new method. Results of this application proved that the continuity of the events is fully preserved while there are no gaps in the diffraction events, even where they intersect other events. The final image obtained by this method on real data showed successful CO-CDS imaging in complex media. As a byproduct, attributes obtained by CO-CDS, have several applications. They can be used for velocity model determination, time or depth migration, for stacking PP waves and PS conversions from multicomponent data.

Key words: CRS, CDS, CO-CDS, seismic imaging, complex structures, conflicting dips

1. INTRODUCTION

The objective of seismic reflection imaging is to provide an image of the subsurface from multicoverage seismic reflection data by enhancing genuine reflection signals and suppressing unwanted energy in the form of coherent and random noise (Robein 2010). The importance of high quality section for geological interpretation is one of the most important tools for any interpreter. It is especially a crucial task in complex structures (Soleimani et. all, 2010a) In many imaging techniques an appropriate macro velocity model is needed in order to calculate further parameters and make geological section to interpret, (Berkovitch, 2008). Hubral (1999) derived a velocity model independent description of travel times in the vicinity of a chosen central ray that was later extensively used for imaging in complex structures, (Heilmann, 2007; Leite et al. 2010; Soleimani et al. 2010b). This traveltime formula depends on three parameters and can be considered as the reflection response of a circular reflector mirror segment, the so-called common-reflection-surface (CRS). Müller (1998) introduced the CRS method as a zero offset (ZO), simulation technique for 2D data which does not require an explicit knowledge of the macro-velocity model. For the 2D case, the shape of the operator depends on three parameters and can be considered as the approximate reflection response of a circular reflector mirror segment, the so-called CRS (Jäger et. al. 2001), (figure 1a). Any contributions along any realization of this operator are tested by means of coherence analysis for each ZO sample, (Hertweck, 2004). The CRS equation with its three attributes reads (Jäger, 1999):

$$t_{hyp}^2(x_m,h)=\left[t_0+\frac{2\sin\alpha(x_m-x_0)}{v_0}\right]^2 + \frac{2t_0\cos^2\alpha}{v_0}\left[\frac{(x_m-x_0)^2}{R_N}+\frac{h^2}{R_{NIP}}\right] \quad (1)$$

Where R_{NIP} is the radius of the normal incidence point (NIP) wave, R_N is the radius of the normal wave, and α is emergence angle of the normal ray. The three kinematic stacking attributes are data-derived wavefield properties that characterize parameters related to the normal ray. The idealized CRS operator which has been built with all common reflection point (CRP), trajectories takes much larger part of the multi coverage dataset into account than CRP trajectory (figure 1b).

2. THE CO CRS STACK METHOD

Höcht (1998) showed that the CRS stacking operator approximates events in the prestack data much better than conventional stacking operators as used. Furthermore, in contrast to certain conventional imaging methods as, e.g., the common midpoint (CMP) stack, the CRS stack makes use of the full multicoverage data volume during the imaging process, (Yang et. al. 2012). As a generalization of the ZO-CRS stack method, Zhang et al., (2001) and Bergler, (2001) introduced a new hyperbolic traveltime approximation, parameterized by five kinematic attributes. This traveltime approximation defines a stacking operator for simulating any common offset (CO), stacked section from multi-coverage dataset. The CO-CRS stacking operator approximates finite-offset (FO) reflection events in the vicinity of a given FO central ray, (Baykulov, 2009). This CO stacking method has been applied for stacking primary reflection of PP or SS waves or converted PS or SP waves. Hyperbolic traveltime T(Δx, Δh) for CO-CRS is (Bergler, 2001):

$$t^2(\Delta x_m,\Delta h)=\left[t_o+\left(\frac{\sin\beta_G}{v_G}+\frac{\sin\beta_S}{v_S}\right)\Delta x_m+\left(\frac{\sin\beta_G}{v_G}-\frac{\sin\beta_S}{v_S}\right)\Delta h\right]^2 + 2t_0\left[\begin{array}{l}\Delta x_m\left(K_3\frac{\cos^2\beta_G}{v_G}+K_3\frac{\cos^2\beta_S}{v_S}\right)\Delta h \\ +\frac{1}{2}\Delta x_m\left((4K_1-3K_3)\frac{\cos^2\beta_G}{v_G}-K_2\frac{\cos^2\beta_S}{v_S}\right)\Delta x \\ -\frac{1}{2}\Delta h\left(K_3\frac{\cos^2\beta_G}{v_G}-K_2\frac{\cos^2\beta_S}{v_S}\right)\Delta h_m\end{array}\right] \quad (2)$$

Where K_1 is the wavefront curvature of the emerging wave at the surface at receiver position in the common shot data, K_2 and K_3 are the wavefront incident at the source and receiver in the CMP data, respectively. The parameters β_S and β_G are emergence angle of the central ray in shot and receiver, respectively. These parameters are better shown in figure 2. For the illustration of both experiments, the wavefronts are depicted by circular segments with the corresponding curvature of the wavefront at the central ray.

The five wave fields attributes K_1, K_2, K_3, β_S and β_G have to be computed. The wavefield attributes are important values which can be used for further calculations. They are related to the elements of the surface-to-surface ray propagator matrix. Thus, one can compute by means of the attributes the geometrical spreading factor and the projected Fresnel zone, (Vieth, 2001).

The CO CRS method has the same advantages as outlined above. Firstly, the five-parametric CO CRS stacking operator is macro model independent and also fully automatically obtained by means of a coherency analysis. Secondly, the parameterization of the operator is based on a model of curved interfaces and, therefore, fits the actual reflection event in the prestack data very well. And thirdly, the stacking operator uses the full multicoverage data volume during the imaging process.

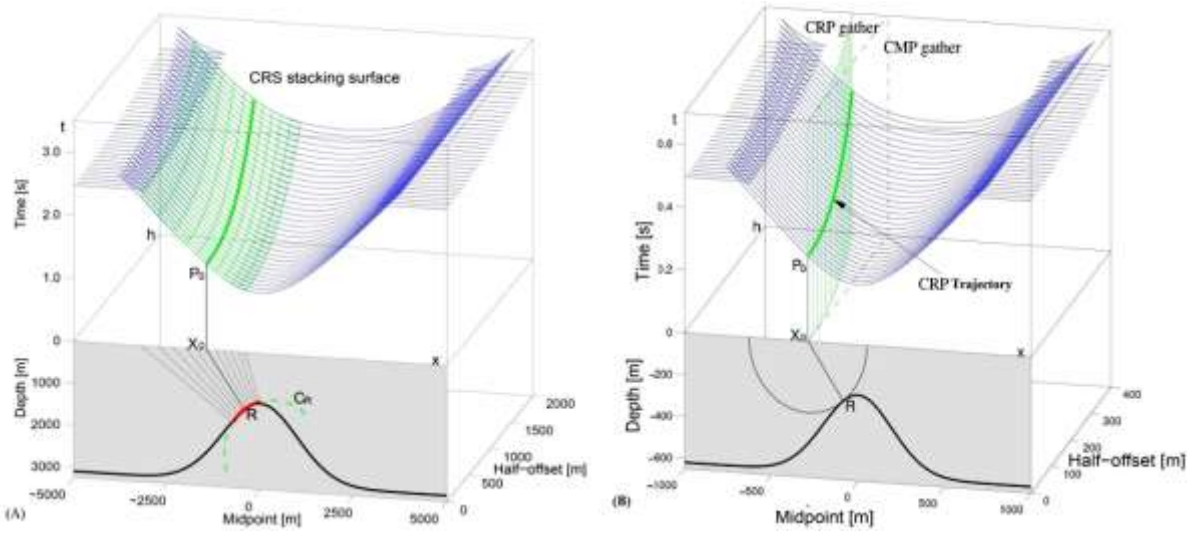

Fig. 1: (A) operator of the common reflection surface. Top: the green surface is the CRS tangent with the blue CO travel time surface. Bottom: the red line shoes the reflector shot related to the green CRS. The curvature of the reflector is estimated by the green circle with the radius of C_R. (B) the common reflection point trajectory used for conventional NMO correction. (Jäger, 1999).

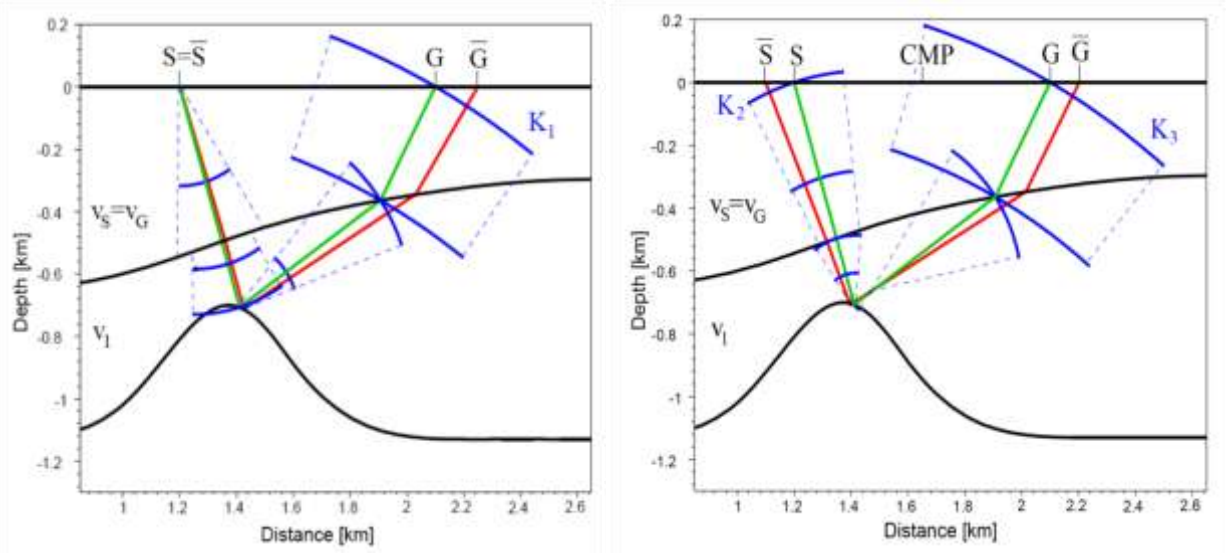

Fig. 2: Two experiments in an isotropic model with constant-velocity layers. For both experiments, the central ray is depicted in green, and the paraxial ray is shown in red. K_1 is the emerging wave at the surface at G in the common shot experiment. K_2 and K_3 are the wavefront emerging at the receiver the source S and the receiver G in the CMP experiment, respectively, (Bergler. 2001).

3. THE CDS STACK IMAGING METHOD

In the CRS stack method, the same idea as dip move-out (DMO) was used to derive a travel time equation for imaging in complex structures and/or to resolve the problem of conflicting dips, the so called common diffraction surface (CDS) stack method (Soleimani et. al, 2009, Soleimani and Mann, 2009). The shape of the CDS operator in time domain is just like the CRS operator with the difference that in general, asymmetrically distributed pairs of shot and receivers will contribute into stacking for one sample. The number of conflicting dips is not of interest here, because any present dip will contribute into stacking for the sample in stack section. This method will enhance the usually weak diffraction events in the stacked section that previously were covered by other events. For reflection events, this implies a less accurate approximation than the full CRS operator (1), but for a fixed emergence angle α, the only attribute to be searched for is a combination of R_{NIP} and R_N, called the R_{CDS}. So the equation of the CRS will reduce to (Soleimani et. al. 2009):

$$t_{hyp}^2(x_m,h)=\left[t_0+\frac{2\sin\alpha(x_m-x_0)}{v_0}\right]^2 + \frac{2t_0\cos^2\alpha}{v_0 R_{CDS}}\left[(x_m-x_0)^2+h^2\right] \quad (3)$$

By considering all possible angles in equation (3), a set of operators will make a weighted volume for each ZO sample. In the producing the CDS operator, the first thing that should be defined by the user is the range of the considered emergence angles along with a suitable angle increment. The larger the search range the more computation time is needed to define the individual operators. The target zone, the aperture, and the range for minimum and maximum stacking velocity should be defined , too. Now, by knowing the optimum value of R_{CDS} and the emergence angle α, equation (3), defines the shape of the stacking operator for the specified sample.

4. Introducing concepts of the CO-CDS

In the CO-CDS stack method, the same idea as DMO was used to overcome the problem of conflicting dips (Hale, 1991). For each sample, a coherence analysis is done for a range of angles. In the CO section, the operator often encounters intersections of reflection and diffraction events. Resolving the problem of conflicting dips will enhance the usually weak diffraction events in the stacked section. For a diffraction point at depth, it is assumed that the incident wave propagates along the central ray. Perroud et. al. (1997) showed that the rays paraxial to the central ray considered for any configuration (CS, CR, CO, CMP) can be associated with certain real (CS, CR) and hypothetical (CO, CMP) wavefronts propagating from source to receiver. However, construction of the simulated time migration CO section requires the diffraction-stack traveltime equation for that diffraction point. This traveltime equation provides an approximation of what is occasionally called the Cheops pyramid. The intersection of the CDS operator in CO mode with the Cheops pyramid requires that the $K_G^{CMP}=K_G^{CS}$ or $K_1 = K_3$. Each sample in the CO section will receive contributions from any possible optimum operator for each angle that is searched for.

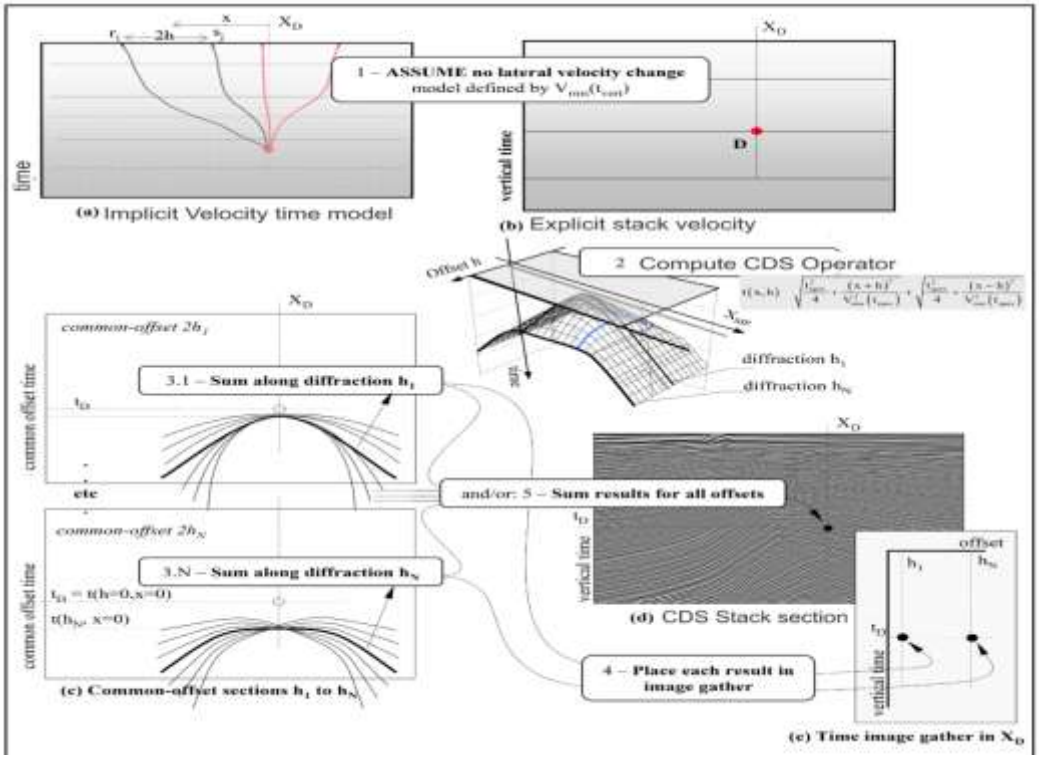

Fig. 3: Processing steps of the Common Offset Common Diffraction Surface (CO-CDS) stack method. The CDS Operator is made for each offset that is produced by many diffraction curves all with a same predefined velocity but different angle of incidence for central ray, (modified by authors after Robein, 2003).

Obviously, this not only increases the signal-to-noise ratio, but also enhances any weak reflection and diffraction events which were obscured by dominant coherent events:

$$t^2(\Delta x_m,\Delta h)=\left[\begin{array}{l} t_o+\left(\frac{\sin\beta_G}{v_G}+\frac{\sin\beta_S}{v_S}\right)\Delta x_m \\ +\left(\frac{\sin\beta_G}{v_G}-\frac{\sin\beta_S}{v_S}\right)\Delta h \end{array}\right]^2 \qquad (4)$$
$$+2t_0\left[\begin{array}{l} \Delta x_m\left(K_3\frac{\cos^2\beta_G}{v_G}+K_3\frac{\cos^2\beta_S}{v_S}\right)\Delta h \\ +\frac{1}{2}\Delta x_m\left(K_1\frac{\cos^2\beta_G}{v_G}-K_2\frac{\cos^2\beta_S}{v_S}\right)\Delta x_m \\ -\frac{1}{2}\Delta h\left(K_3\frac{\cos^2\beta_G}{v_G}-K_2\frac{\cos^2\beta_S}{v_S}\right)\Delta h_m \end{array}\right]$$

Figure 3 shows the processing steps of the CO-CDS stack method. In these steps, a CDS stacked section for each offset section is obtained by CO-CDS stack method. Then all of these sorted offset sections could be stacked by conventional stacking method to produce a zero offset CDS stacked section, (figure 4).

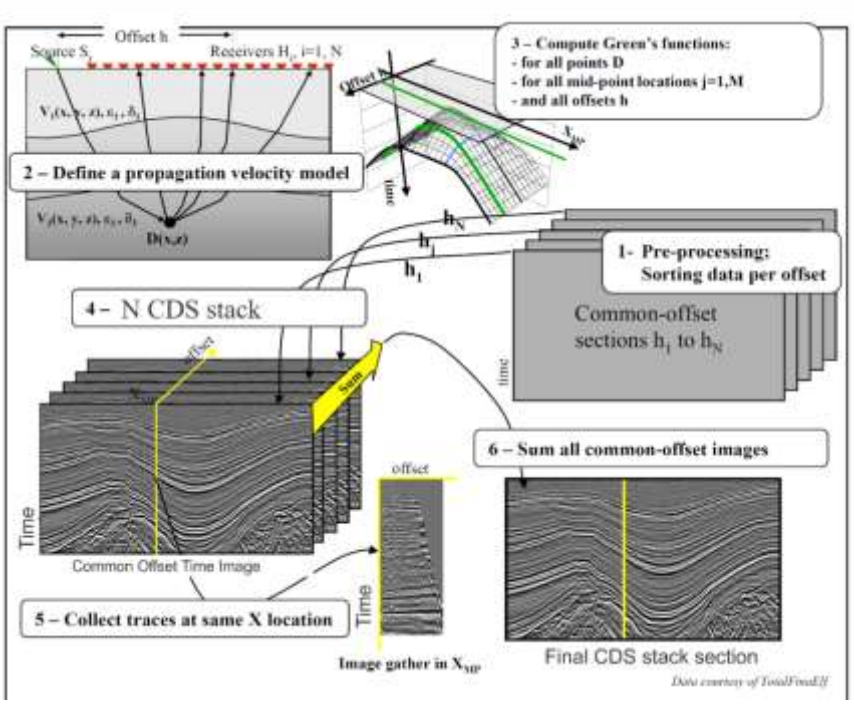

Fig. 4: All the common offset sections were prepared by CO-CDS stack method, now ready to be stacked by conventional stack process, (modified by authors after Robein, 2003).

5. APPLICATION OF CO-CDS ON THE SIGSBEE 2A SYNTHETIC DATA

Sigsbee 2A is a constant density acoustic synthetic data set that consists of a salt body with very complex geometry. In this study, we used only the horizontal layer parts with numbers of faults in it, (Figure 5a). This part was only used to see whether the partial CDS stack can image more diffractions than the other methods. Imaging much more diffraction energy was the final goal here, while it should be investigated that if the partial CDS method could resolve the problem of conflicting dips or not. If the method gave promising results, then it could be applied with more confidence on semi-complex or complex data. To show the advantages of applying the partial CDS to a noisy data set, random noise with S/N=5 was added to the synthetic data. Result of application the CO-CRS method, the extended search strategy and the CO-CDS method are shown in figure 5b-d, respectively.

.

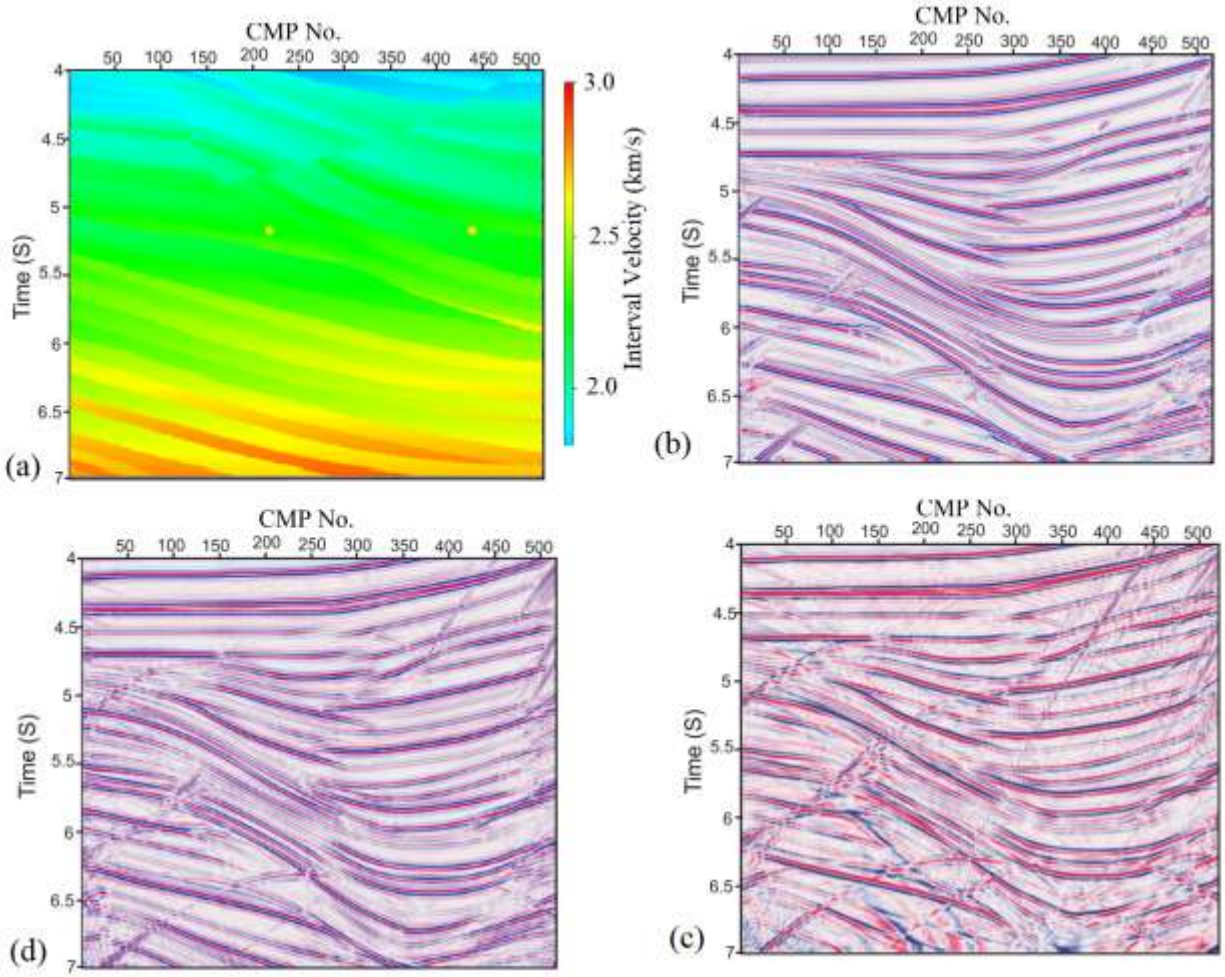

Fig. 5- (a): Sigsbee 2A data, true interval velocity model (b), CO-CRS section, (c) extended search strategy and the CO-CDS section.

The CO-CRS stack and the extended search strategy methods could also resolve the problem of conflicting dips, but more diffraction events were obviously imaged with the CO-CDS method. The result of the CO-CDS method, as was mentioned before, shows higher lateral resolution while tails of diffraction events (especially the large diffraction starting at CDP number 450) are also imaged only in this section. Diffraction patterns also are enhanced in all parts of this section. Particularly, in the sedimentary structures in the left-hand part of the section, diffraction events which are partly or fully obscured by reflection events in the other results are all imaged by the CO-CDS method. In the section related to the extended search strategy, diffraction patterns are simulated, too, but some of them have gaps where they intersect reflection event. These gaps correspond to the locations where the conflicting dip situations have not been properly detected during the stack.

6. APPLICATION OF CO-CDS ON A LAND DATA SET

The Gorgan region is located in the North East of Iran, east of the Caspian Sea. In most of the seismic surveying in this area, the mud volcanoes play an important role for planning the seismic surveying line. Therefore, defining the boundary of mud volcanoes is one of the difficulties in interpreting seismic time or depth sections from such regions. The partial CDS and partial CRS methods were applied on a real 2D data set containing three mud volcanoes. The data suffer from linear noise, air blast noise, ground roll and random noise. As was mentioned before, the CDS and partial CDS methods will enhance any weak diffraction events in pre-stack data. Therefore, in such data with lots of coherent noise, care needs to be taken to suppress the noise up front as much as possible. Therefore, the data underwent careful preprocessing operations, such as: geometry correction, static correction (with refraction tomography), various noise attenuation techniques, amplitude recovery and pre-stack spectrum widening with bandwidth extension (BE with continues wavelet transform, CWT) method. Table 1 shows general parameters used for processing by the partial CRS and partial CDS methods. Figure

6a and 6b shows depth migration results of the CO- CRS and CO-CDS methods, respectively. Figure 7 also shows the velocity model used for depth migration.

The velocity model used for migration was obtained by NIP tomography, see Duveneck (2004) for details. The migrated sections show a layered medium at the top (from surface to depth 2000 m in the left part and 4000 m in right part). At the bottom of the section, there are three mud volcanoes (horizontal positions of their apexes are at CDPs 400, 600 and 1200, respectively). These mud volcanoes are highlighted by black rectangles in figure 6b. The CO-CDS operator gathers more energy that might not be taken into account by the other methods. Therefore, more events with more details are imaged in the final migrated section of CO-CDS data. The boundaries of the mud volcanoes can be detected better and the faults in the upper right are also imaged well. The reflectors and the other structures produced diffraction events, like as body of mud volcanoes and faults could be seen clearly here in this section. In CO-CDS enhanced section, the wedges between CDPs 800 to 1100 below the unconformity are imaged well. Finally, it could be said that in a semi-complex structure data, the migrated section of CO-CDS better focuses the energy of diffraction events. Therefore, it shows better the truncation of the reflectors at the body of the mud volcanoes. These events are all shown in subsections in figure 8. Structural events (faults and body of mud volcano) are better imaged by migration of CO-CDS data, shown in figure 8b.

Table 1- Processing parameters used for partial CRS and partial CDS methods of real data with mud volcano.

Context	Processing parameters	Setting
General parameters	Dominant frequency	30 Hz
	Coherence measure	Semblance
	Data used for coherence analysis	Original traces
	Temporal width of coherence band	56 ms
Velocity and constraints	Near surface velocity	1500 m/s
	Tested stacking velocity	1500 to 5000 m/s
Target zone	Simulated ZO traveltime	0 to 7 s
	Simulated temporal sampling intervals	4 ms
	Number of simulated ZO traces	1.8×10^4
	Spacing of simulated ZO traces	17.5 m
Partial CDS parameters	Tested emergence angle	-60 to +60 degree
	Initial emergence angle increment	1 degree
	Factor of CS search sampling rate	2 ms
	Number of iterations in CS search	3

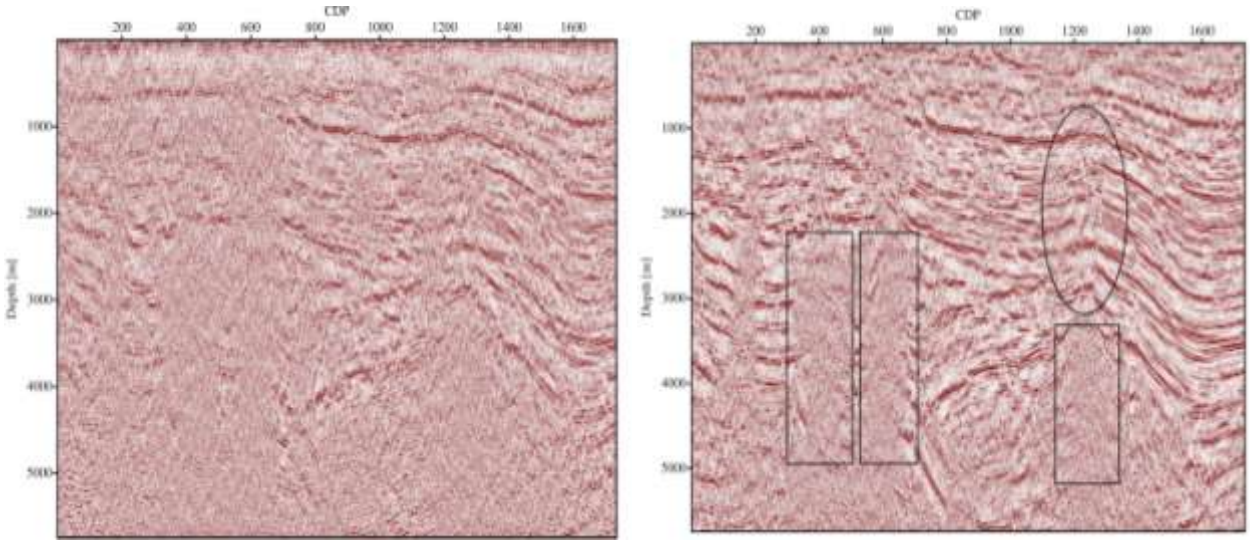

(a) **(b)**

Fig. 6- (a) Migrated section of the CO-CRS data and (b) migrated section of the CO-CDS enhanced data in area with mud volcano. Fault zone is shown in ellipse and mud volcanoes by rectangles.

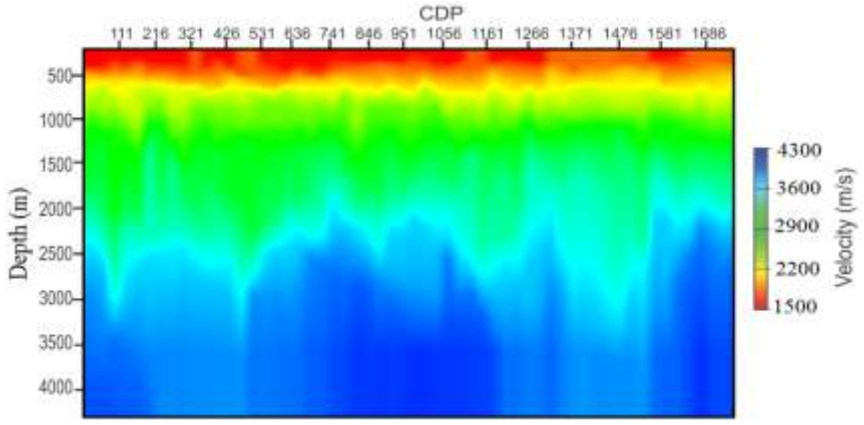

Fig. 7- The velocity model used for depth migration of CO-CRS and CO-CDS in area with mud volcano.

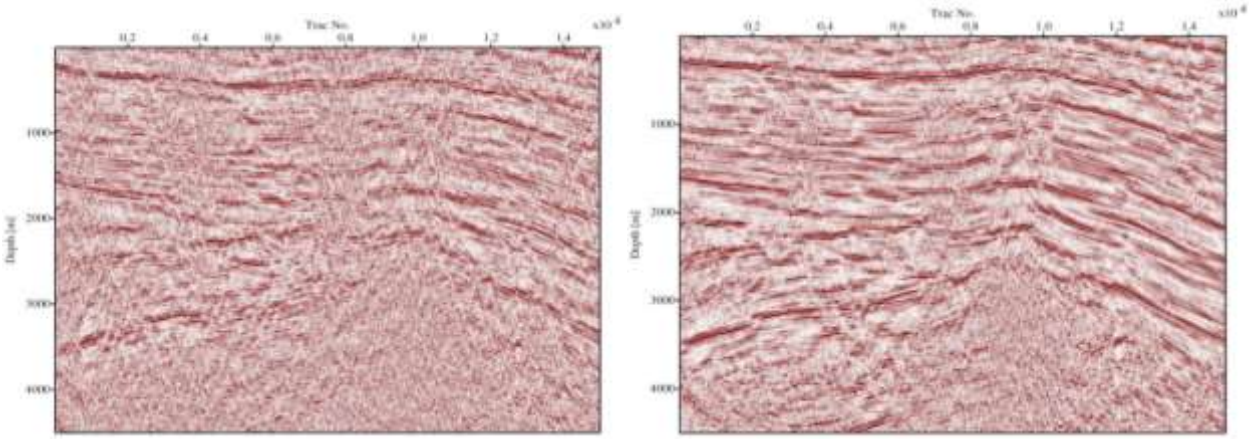

(a) **(b)**

Fig. 8- (a) Subsection of migrated section of the CO-CRS and (b) the same subsection CO-CDS data in area with mud volcano.

Common image gathers, (CIG) are widely used for correction checking of the velocity model. It is obvious that events in CIGs should be flat, that proves same depth for each reflector in different offsets. Some common image gathers of the data were collected for visual checking, (figure 9). Horizontal events in both common image gathers indicate good consistency and accuracy of the velocity model used for migration. However, in the CIGs obtained from migration of CO-CDS enhanced data, more horizontal events are shown while more energy are gathered.

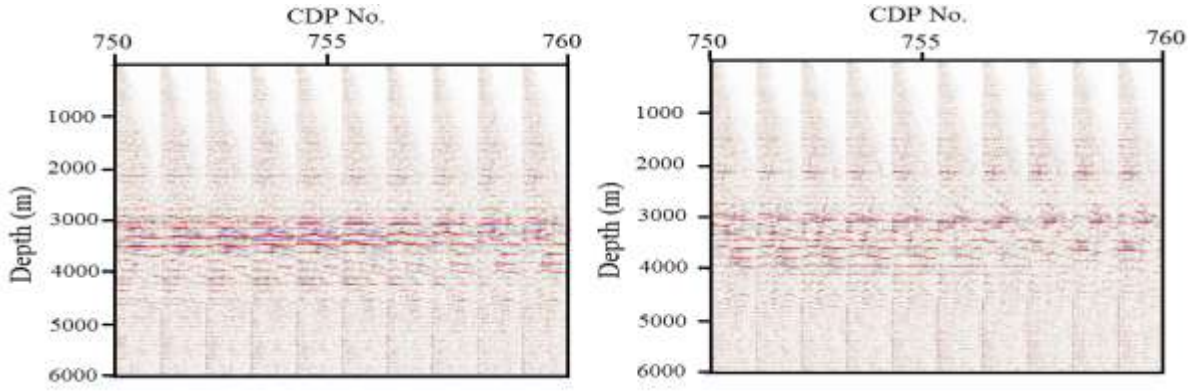

(a) **(b)**

Fig. 9- Samples of common image gathers (CIGs) to show the consistency of velocity model with data and depth migrated results. (a) CIGs from CO-CDS results and (b) CIGs from CO-CRS results.

CONCLUSIONS

The Common Offset CDS method stack introduced here to overcome some of the problem of seismic imaging in complex geological structures. The result of the CO-CDS stack showed that it can serve as a method for imaging in complex structures. This mainly relates to the stacking operator that gathers most of the energy in data that relates to a diffraction point in depth. The CO-CDS operator enhances weak events that were previously covered by dominant events in other methods. These events are mostly diffraction events that are related to a structure like faults or mud volcano bodies. This method was applied on synthetic and real data sets. After conventional processing, data set was processed by the CO-CRS and the CO-CDS stack methods. The stacked sections showed that the CO-CDS method can clearly define the boundary of mud volcano that was not imaged well by other methods. The near surface faults and the larger fault that was continued to larger times were also imaged better in the migrated section of the CO-CDS stacked result. Therefore, it could be said that the CO-CDS operator volume stacked section provides suitable input for migration in complex media.

REFERENCES

[1]. Baykulov, M. (2009), Seismic imaging in complex media with the Common Reflection Surface stack. Ph. D Thesis, Hamburg University.
[2]. Berkovitch A., Belfer I., and Landa, E. (2008), Multifocusing as a method of improving subsurface imaging. The Leading Edge, 27, 250–256. DOI:10.1190/1.2840374.
[3]. Bergler, S.(2001), The Common-Reflection-Surface Stack for Common Offset - Theory and Application. Master's thesis, University of Karlsruhe.
[4]. Duveneck, E., (2004), Velocity model estimation with data-derived wavefront attributes. Geophysics, 69, 265–274.
[5]. Hale, D. (1991), Dip moveout processing. Society of Exploration Geophysics, Tulsa.
[6]. Heilmann, Z. (2007), CRS-stack-based seismic reflection imaging for land data in time and depth domain. Logos Verlag, Berlin.
[7]. Hertweck, T. (2004), True-amplitude Kirchhoff migration: analytical and geometrical considerations. Logos Verlag, Berlin.
[8]. Höcht, G. (1998), The Common Reflection Surface stack. Master's thesis, University of Karlsruhe.
[9]. Hubral, P. (1999), Macro-model independent seismic reflection imaging. Journal of Applied Geophysics 42.
[10]. Jäger, R. (1999), The Common Reflection Surface stack - theory and application. Master's thesis, University of Karlsruhe.
[11]. Jäger, R., Mann, J., Höcht, G., and Hubral, P. (2001), Common-reflection-surface stack: Image and attributes. Geophysics 66, 97–109. DOI:10.1190/1.1444927.
[12]. Leite, L.W.B., Lima, H.M., Heilmann, B.Z. and Mann, J. (2010), CRS-based Seismic Imaging in Complex Marine Geology, 72nd EAGE Conference & Exhibition, Barcelona, Spain, P396.
[13]. Perroud, H., Hubral, P., Höcht, G., and de Bazelaire, E. (1997), Migrating around in circles - part III. The Leading Edge, 16(6):875–883.
[14]. Müller. T. (1998), "common reflection surface stack versus NMO/DMO/stack." 60th Conf. Eur. Assn. Geosci. Eng. Session B040.
[15]. Robein, E. (2003), Velocities, time imaging and depth imaging in reflection seismic, principles and methods. Eur. Assn. Geosci. Eng. Press. Netherlands.
[16]. Robein, E. (2010), Seismic imaging. Eur. Assn. Geosci. Eng. Press. Netherlands.
[17]. Soleimani, M., Piruz, I., Mann, J. and Hubral, P., (2009), Common-Reflection-Surface stack: accounting for conflicting dip situations by considering all possible dips. Journal of Seismic Exploration 18, 271-288.
[18]. Soleimani, M. and Mann, J. (2009), Merging aspects of DMO correction and CRS stack to account for conflicting dip situation." 12th Wave Inversion Technology (WIT) Meeting, Hamburg, Germany.
[19]. Soleimani, M., Mann, J., Adibi, E., Shahsavani, M., and Piruz, I. (2010a), Applying the CRS stack method to solve the problem of imaging of complex structures in the Zagros overthrust, south west Iran. 72nd EAGE Conference & Exhibition. Barcelona, Spain, P556.
[20]. Soleimani, M. Mann, J., Adibi, E. and Piruz, I. (2010b), Improving the seismic image quality in semi-complex structures in north east Iran by the CDS stack method." 72th EAGE , Barcelona,. Extended Abstracts.
[21]. Vieth, K., U. (2001), Kinematic wavefield attributes in seismic imaging. Logos verlag, Berlin.
[22]. Yang, K., Bao-shu Chen, B. S., Wang, X., J., Yang, X., J., and Liu, J. R. (2012), Handling dip discrimination phenomenon in common-reflection-surface stack via combination of output-imaging-scheme and migration/demigration. Geophysical Prospecting, 60, 255–269.
[23]. Zhang, Y., Bergler, S., and Hubral, P. (2001), Common-reflection-surface (CRS) stack for common offset. Geophysical Prospecting, 49, 709-718.